

# Absorption spectra for strong pump and probe in atomic beam of cesium atoms

T. Zigdon, A. D. Wilson-Gordon, and H. Friedmann  
*Department of Chemistry, Bar-Ilan University, Ramat Gan 52900, Israel*  
 (Received 5 April 2009; published 16 September 2009)

We calculate the pump and probe absorption spectra for the cycling  $F_g=4 \rightarrow F_e=5$  transition  $D_2$  line of  $^{133}\text{Cs}$  in an atomic beam, interacting with a strong resonant  $\sigma_+$ -polarized pump and a probe of comparable intensity and either  $\sigma_-$  or  $\pi$  polarization. The aim is to reproduce and analyze the experiments of Dahl *et al.* [Opt. Lett. **33**, 983 (2008)] who showed for a  $\sigma_+$ -polarized pump and  $\sigma_-$ -polarized probe that the pump absorption spectrum switches from an “absorption within transparency” (AWT) structure, when the probe is weaker than the pump, to a “transparency within transparency” (TWT) structure, when the probe is stronger than the pump. For all other polarization combinations, the pump spectrum displays AWT behavior at all probe intensities. We analyze our results by considering the contributions that derive from the individual  $m_g \rightarrow m_e$  transitions. When the  $\sigma_+$ -polarized pump is stronger than the  $\sigma_-$ -polarized probe, the population is swept toward the  $m_g \rightarrow m_e = m_g + 1$  transitions with the highest values of  $m_g$ , and the pump absorption spectrum has an AWT structure and resembles that of an  $N$  system. However, when the probe is stronger than the pump, the population is swept toward the  $m_g = -F_g \rightarrow m_e = m_g - 1$  transition when the probe is near resonance, and to the  $m_g = F_g \rightarrow m_e = m_g + 1$  transition when the probe is detuned from resonance. The pump and probe spectra are mirror images of each other and resemble those of a  $V$  system where the probe has a peak at line center and the pump spectrum has a TWT structure. For a strong  $\sigma_+$  pump and an even stronger  $\pi$  probe, the population concentrates in the intermediate transitions, and the AWT to TWT changeover does not occur. We also show that the narrow features in the spectra at line center derive from transfer of coherence from the excited to the ground hyperfine levels.

DOI: [10.1103/PhysRevA.80.033825](https://doi.org/10.1103/PhysRevA.80.033825)

PACS number(s): 42.50.Gy, 42.50.Hz

## I. INTRODUCTION

In a previous paper [1], we developed a strategy for calculating the absorption spectra for a degenerate two-level transition interacting with a perpendicularly polarized pump and probe, for the case where the probe intensity is high enough to affect the pump absorption. In particular, we used the theory to calculate the pump and probe absorption spectra, as a function of the probe detuning, for the degenerate  $F_g=2 \rightarrow F_e=3$  transition in the  $D_2$  line of  $^{87}\text{Rb}$ , interacting with a resonant  $\sigma_+$ -polarized pump and either a  $\pi$ - or  $\sigma_-$ -polarized probe. We showed [1] that both the probe and pump absorption spectra are characterized by a narrow electromagnetically induced absorption (EIA) peak at line center [2,3], for the case where  $\Omega_1 \geq \Omega_2 < \Gamma$  ( $\Omega_{1,2}$  are the pump and probe Rabi frequencies and  $\Gamma$  is the rate of spontaneous decay from  $F_e$  to  $F_g$ ) but show complementary behavior in the wings of the spectrum. By contrast, we found that the pump and probe absorption spectra are mirror images of each other when  $\Omega_1 \geq \Omega_2 > \Gamma$ . In order to interpret these results physically, we analyzed the probe and pump absorption spectra in terms of the contributions that derive from the individual  $m_g \rightarrow m_e$  transitions. We then showed how these contributions depend on the ground- and excited-state populations and Zeeman coherences, and investigated the role played by transfer of coherence (TOC) from the excited to ground hyperfine states [4,5] in determining the probe and pump spectra.

Recently, Dahl *et al.* [6] reported measurements of the pump and probe absorption spectra for the degenerate  $F_g=4 \rightarrow F_e=5$  transition in the  $D_2$  line of  $^{133}\text{Cs}$  in an atomic beam, for several combinations of perpendicular pump and

probe polarizations (see, also Spani Molella *et al.* [7]). In all the cases studied [6], the resonant pump Rabi frequency was chosen so that  $\Omega_1 > \Gamma$  and the pump and probe absorption spectra were measured for various values of  $\Omega_2$ , ranging from values less than  $\Omega_1$  to values greater than it. For each combination of polarizations, apart from a  $\sigma_+$ -polarized pump and a  $\sigma_-$ -polarized probe, the pump spectrum was characterized at all probe intensities by a sharp absorption peak at line center within a broader transparency dip which the authors called “absorption within transparency” (AWT). For the  $\sigma_+$  pump and  $\sigma_-$  probe combination, the pump spectrum displayed AWT behavior as long as  $\Omega_2 < \Omega_1$ . However, as the probe intensity was raised so that  $\Omega_2 > \Omega_1$ , the central sharp peak changed into a sharp dip, still within a transparency dip. This structure was called “transparency within transparency” (TWT) by the authors [6].

In this paper, we demonstrate that we cannot only reproduce these results numerically but also offer a detailed physical explanation for them. In order to do so, we compare two polarization combinations:  $\sigma_+$  pump and  $\sigma_-$  probe [see Fig. 1(a)] where the AWT to TWT changeover takes place, and  $\sigma_+$  pump and  $\pi$  probe [see Fig. 1(b)] where the pump spectrum retains AWT behavior even when  $\Omega_2 \gg \Omega_1$ . We show for the  $\sigma_+$  pump and  $\sigma_-$  probe that, when  $\Omega_2 < \Omega_1$ , the population is swept toward the right of the level diagram so that the pump absorption spectrum resembles that of an  $N$  system. However, at line center, there is some population in the extreme left transition leading to a dip in the probe absorption. When  $\Omega_2 > \Omega_1$ , the population at line center is swept toward the extreme left transition when the probe is at resonance, and toward the extreme right transition when the probe is detuned. The pump and probe spectra are mirror images of each other and resemble those of an effective  $V$

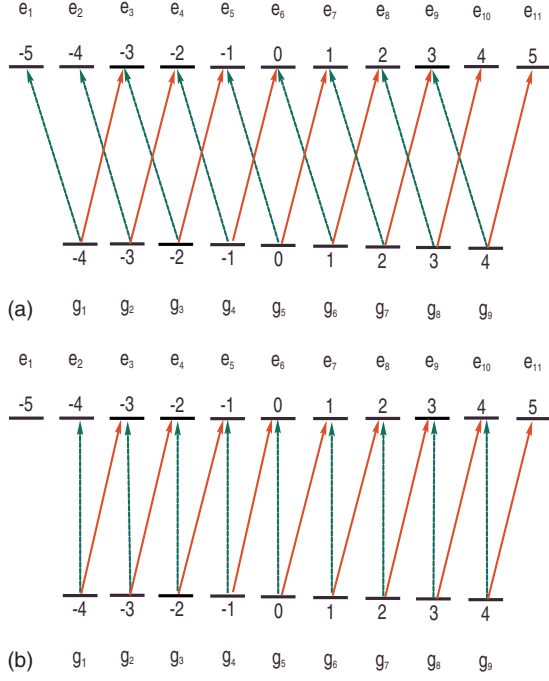


FIG. 1. (Color online) Energy level diagram for  $F_g=4 \rightarrow F_e=5$  transition interacting with  $\sigma_+$ -polarized pump and (a) a  $\sigma_-$ -polarized probe, and (b) a  $\pi$ -polarized probe.

system where the probe has an EIA peak at line center and the pump spectrum has a TWT structure. For the case of a  $\sigma_+$  pump and  $\pi$  probe, the population concentrates nearer the center of the energy-level diagram as  $\Omega_2$  increases, rather than in the extreme left and right transitions, as in the case of a  $\sigma_-$ -polarized probe. Thus the pump spectrum never exhibits a changeover to TWT. It should be noted that the Doppler effect is largely avoided in the atomic beam spectra examined by Dahl *et al.* [6] so that averaging over the molecular velocity distribution can be omitted in the calculation of these spectra.

## II. PUMP AND PROBE ABSORPTION

The Bloch equations (see [1,5]) we use to calculate the absorption spectra for a degenerate two-level system are not reproduced here. However, we do reproduce the equations which allow us to interpret the calculated spectra. The steady-state pump and probe absorption  $\alpha(\omega_{1,2})$  can be expressed in terms of the contributions from the individual  $F_g m_g \rightarrow F_e m_e$  transitions by [8]

$$\alpha(\omega_{1,2}) = \frac{4\pi\omega_0 N}{\hbar c} \sum_{e_i g_j} \frac{|\mu_{e_i g_j}|^2}{V_{e_i g_j}(\omega_{1,2})} \text{Im}[\rho_{e_i g_j}(\omega_{1,2})], \quad (1)$$

where  $N$  is the density of atoms and  $\omega_0$  is the frequency of the ground- to excited-state transition in the absence of a magnetic field,  $\omega_{1,2}$  are the pump and probe frequencies, and  $V_{e_i g_j}(\omega_{1,2})$  are the pump and probe Rabi frequencies for the individual  $F_g m_g \rightarrow F_e m_e$  transitions, given by

$$2V_{e_i g_j}(\omega_{1,2}) = \frac{2\mu_{e_i g_j} E_{1,2}}{\hbar} = (-1)^{F_e - m_e} \begin{pmatrix} F_e & 1 & F_g \\ -m_e & q & m_g \end{pmatrix} \Omega_{1,2}, \quad (2)$$

where  $E_{1,2}$  are the pump and probe electrical field amplitudes,  $\Omega_{1,2} = 2\langle F_e || \mu || F_g \rangle E_{1,2} / \hbar$  are the general pump and probe Rabi frequencies for the  $F_g \rightarrow F_e$  transition and  $q = (-1, 0, 1)$  depending on the selection rules which are determined by the polarization of the incident laser. The dipole moment is calculated from [9]

$$\mu_{e_i g_j} = \sqrt{\frac{3c^3 \hbar \Gamma}{4\omega_{e_i g_j}}} (-1)^x \sqrt{2J_e + 1} \sqrt{2F_e + 1} \sqrt{2F_g + 1} \times \begin{Bmatrix} F_e & 1 & F_g \\ J_g & I & J_e \end{Bmatrix} \begin{pmatrix} F_e & 1 & F_g \\ -m_e & q & m_g \end{pmatrix}, \quad (3)$$

where  $x = 1 + I + J_e + F_e + F_g - m_e$  and  $c$  is the speed of light in vacuum.

In Eq. (1), we see that the total spectrum is the sum of contributions from the individual  $F_g m_g \rightarrow F_e m_e$  transitions. It is very instructive to study the spectra of the individual transitions and their contribution to the total spectrum. In this way, we can often show that the total spectrum derives mainly from a subset of the individual transitions. Often these subsets can be characterized in terms of simple two-, three-, or four-level systems, whose spectral features are well known [10]. The spectrum of the individual transitions can, in turn, be decomposed into terms that derive from the ground- and excited-state populations and Zeeman coherences. By studying these contributions, further insight can be obtained especially with regard to the role of TOC in determining the spectra.

For the case where the pump is  $\sigma_+$  polarized and the probe  $\sigma_-$  polarized, the density-matrix elements  $\rho_{e_i g_j}(\omega_{1,2})$  for the individual  $F_g m_g \rightarrow F_e m_e$  transitions, can be written as

$$\rho_{e_i g_j}(\omega_1) = [\eta_{e_i g_j}(\omega_1) - i\kappa_{e_i g_j}(\omega_1)] \{(\rho_{e_i e_i} - \rho_{g_j g_j}) V_{e_i g_j}(\omega_1) + \rho_{e_i e_{i-2}}(\omega_1 - \omega_2) V_{e_{i-2} g_j}(\omega_2) - \rho_{g_{j+2} g_j}(\omega_1 - \omega_2) V_{e_i g_{j+2}}(\omega_2)\}, \quad (4)$$

$$\rho_{e_i g_j}(\omega_2) = [\eta_{e_i g_j}(\omega_2) - i\kappa_{e_i g_j}(\omega_2)] \{(\rho_{e_i e_i} - \rho_{g_j g_j}) V_{e_i g_j}(\omega_2) + \rho_{e_i e_{i+2}}(\omega_2 - \omega_1) V_{e_{i+2} g_j}(\omega_1) - \rho_{g_{j-2} g_j}(\omega_2 - \omega_1) V_{e_i g_{j-2}}(\omega_1)\}, \quad (5)$$

where

$$\eta_{e_i g_j}(\omega_{1,2}) = \frac{\Delta_{e_i g_j}(\omega_{1,2})}{\Gamma_{e_i g_j}' + \Delta_{e_i g_j}^2(\omega_{1,2})}, \quad (6)$$

and

$$\kappa_{e_i g_j}(\omega_{1,2}) = \frac{\Gamma_{e_i g_j}'}{\Gamma_{e_i g_j}' + \Delta_{e_i g_j}^2(\omega_{1,2})}. \quad (7)$$

with

$$\Delta_{e_i g_j}(\omega_{1,2}) = \omega_{e_i g_j} - \omega_{1,2}. \quad (8)$$

The dephasing rates of the excited to ground state optical coherences are given, in the absence of collisions, by  $\Gamma'_{e_i g_j} = \gamma + \Gamma/2$ , where  $\gamma$  is the decay rate from the ground and excited states to a reservoir, due to time-of-flight of atoms through the copropagating laser beams.

For the case where the pump is  $\sigma_+$  polarized and the probe  $\pi$  polarized, we can write

$$\begin{aligned} \rho_{e_i g_j}(\omega_1) = & [\eta_{e_i g_j}(\omega_1) - i\kappa_{e_i g_j}(\omega_1)] \{ (\rho_{e_i e_i} - \rho_{g_j g_j}) V_{e_i g_j}(\omega_1) \\ & + \rho_{e_i e_{i-1}}(\omega_1 - \omega_2) V_{e_{i-1} g_j}(\omega_2) \\ & - \rho_{g_{j+1} g_j}(\omega_1 - \omega_2) V_{e_i g_{j+1}}(\omega_2) \}, \end{aligned} \quad (9)$$

$$\begin{aligned} \rho_{e_i g_j}(\omega_2) = & [\eta_{e_i g_j}(\omega_2) - i\kappa_{e_i g_j}(\omega_2)] \{ (\rho_{e_i e_i} - \rho_{g_j g_j}) V_{e_i g_j}(\omega_2) \\ & + \rho_{e_i e_{i+1}}(\omega_2 - \omega_1) V_{e_{i+1} g_j}(\omega_1) \\ & - \rho_{g_{j-1} g_j}(\omega_2 - \omega_1) V_{e_i g_{j-1}}(\omega_1) \}. \end{aligned} \quad (10)$$

It can be seen from Eqs. (4), (5), (9), and (10), that the density-matrix elements that determine the contributions of the individual transitions to the total absorption spectra are themselves determined by the populations and coherences of the ground and excited Zeeman sublevels. In the case where the pump is  $\sigma_+$  polarized and the probe  $\sigma_-$  polarized, the Zeeman coherences are between nearest next neighbors, whereas when the pump is  $\sigma_+$  polarized and the probe  $\pi$  polarized, they are between nearest neighbors. This reflects the fact (see Fig. 1) that every transition is coupled via its lower level to another transition forming a  $V$  system. This leads to the dependence of the transition matrix element on the coherence between the two upper states of the  $V$  system, which are separated by  $\Delta m=2$  [Fig. 1(a)] or by  $\Delta m=1$  [Fig. 1(b)]. In addition, every transition in Fig. 1 (except the transitions on the extreme left or the extreme right) is coupled via its upper level to another transition forming a  $\Lambda$  system. This leads to the dependence of the transition matrix element on the coherence between the two lower states of the  $\Lambda$  system, which are also separated by  $\Delta m=2$  [Fig. 1(a)] or  $\Delta m=1$  [Fig. 1(b)].

### III. NUMERICAL RESULTS

We note that the numerical calculations were performed for Rabi frequencies that were used in the experiments of Dahl *et al.* [6]. We find the overall shapes of the spectra and the relative widths of the various spectral features to be in qualitative agreement with experiment [6].

#### A. $F_g=4 \rightarrow F_e=5$ transition interacting with $\sigma_+$ -polarized pump and $\sigma_-$ -polarized probe

##### 1. $\Omega_1 > \Omega_2 > \Gamma$

We first discuss the case where the general Rabi frequency of the  $\sigma_+$ -polarized pump  $\Omega_1$  is greater than that of the  $\sigma_-$ -polarized probe  $\Omega_2$ . We consider the case where  $\Omega_1 > \Omega_2 > \Gamma$ . The probe absorption spectrum for  $\Omega_1/\Gamma=5$  and

$\Omega_2/\Gamma=3.5$  as a function of  $\delta/\Gamma$ , where  $\delta=\Omega_2-\Omega_1$  is the pump-probe detuning, shown in Fig. 2(a), is characterized by a small dip at line center. We use the same approach for analyzing this spectrum as in [1]. When the contributions to the absorption that derive from the various transitions are analyzed using Eq. (1), it is found that the main contributions to the total probe absorption [Fig. 2(a)] come from the terms proportional to  $\text{Im}[\rho_{e_1 g_1}(\omega_2)]$  and  $\text{Im}[\rho_{e_9 g_9}(\omega_2)]$ , shown in Figs. 2(b) and 2(c), with smaller contributions of similar shape from the terms proportional to  $\text{Im}[\rho_{e_i g_i}(\omega_2)]$  where  $i=2-4$ , and  $\text{Im}[\rho_{e_i g_i}(\omega_2)]$  where  $i=5-8$ , respectively (not shown). From Figs. 2(b) and 2(c), we see that the main contributions to the total probe absorption, when the probe is detuned from resonance, come from the transitions toward the right, whereas the transitions toward the left also contribute when the probe is at resonance, resulting in a dip at resonance in the total absorption. Using Eq. (5), we now analyze the contributions of the ground- and excited-state populations and coherences to the probe absorption that derives from the  $g_1 \rightarrow e_1$  and  $g_9 \rightarrow e_9$  transitions, shown in Figs. 2(b) and 2(c). These are shown in Figs. 2(e), 2(h), 2(k), 2(f), 2(i), 2(j), and 2(l), respectively. We see that the  $g_1 \rightarrow e_1$  transition is characterized by a dip at line center which arises from the term proportional to the ground state population whose effect is mitigated by the term proportional to the excited-state population, which has the opposite behavior. By contrast, the  $g_9 \rightarrow e_9$  transition is characterized by a peak at line center as a result of the contributions from the ground-state population and coherence, whose effect is mitigated by the contributions from the excited-state population and coherence, which have behavior complementary to that of the ground-state population and coherence.

The pump absorption spectrum, shown in Fig. 3(a) is characterized by an AWT [6]. The spectrum is complementary to the probe spectrum, shown in Fig. 2(a), that is, the pump absorption decreases when the probe spectrum increases [1,11]. The main contribution to the pump spectrum comes from the terms in Eq. (1) proportional to  $\text{Im}[\rho_{e_{11} g_9}(\omega_1)]$  [see Fig. 3(e)] and smaller contributions which modify the spectrum at line center from  $\text{Im}[\rho_{e_i g_j}(\omega_1)]$  where  $i=j+2=8-10$ , shown in Figs. 3(b)–3(d). It should be noted that it is necessary to include all three contributions in order to obtain the peak at line center of the total spectrum. Using Eq. (4), the contributions to the pump spectrum that derive from the individual transitions can be analyzed in the same way as was done for the probe spectrum. We plot the contributions of ground- and excited-state populations and coherences to the spectra of Figs. 3(b)–3(e) in Figs. 3(f), 3(k), 3(p), 3(r), 3(g), 3(l), 3(q), 3(s), 3(h), 3(m), 3(t), 3(i), 3(n), and 3(u), respectively. The sharp features at line center in the individual contributions to the pump absorption derive from the contributions proportional to the populations in sublevels  $g_j$  where  $j=6-8$  and are reinforced by the contributions proportional to the ground-state Zeeman coherences  $\text{Re}[\rho_{g_9 g_7}(\omega_2 - \omega_1)]$  and  $\text{Re}[\rho_{g_8 g_6}(\omega_2 - \omega_1)]$ . In each case, the contributions from the excited-state populations and coherences behave in a manner complementary to those of the ground state.

It is clear from the above discussion that, for this set of Rabi frequencies, the Cs  $F_g=4 \rightarrow F_e=5$  transition cannot be

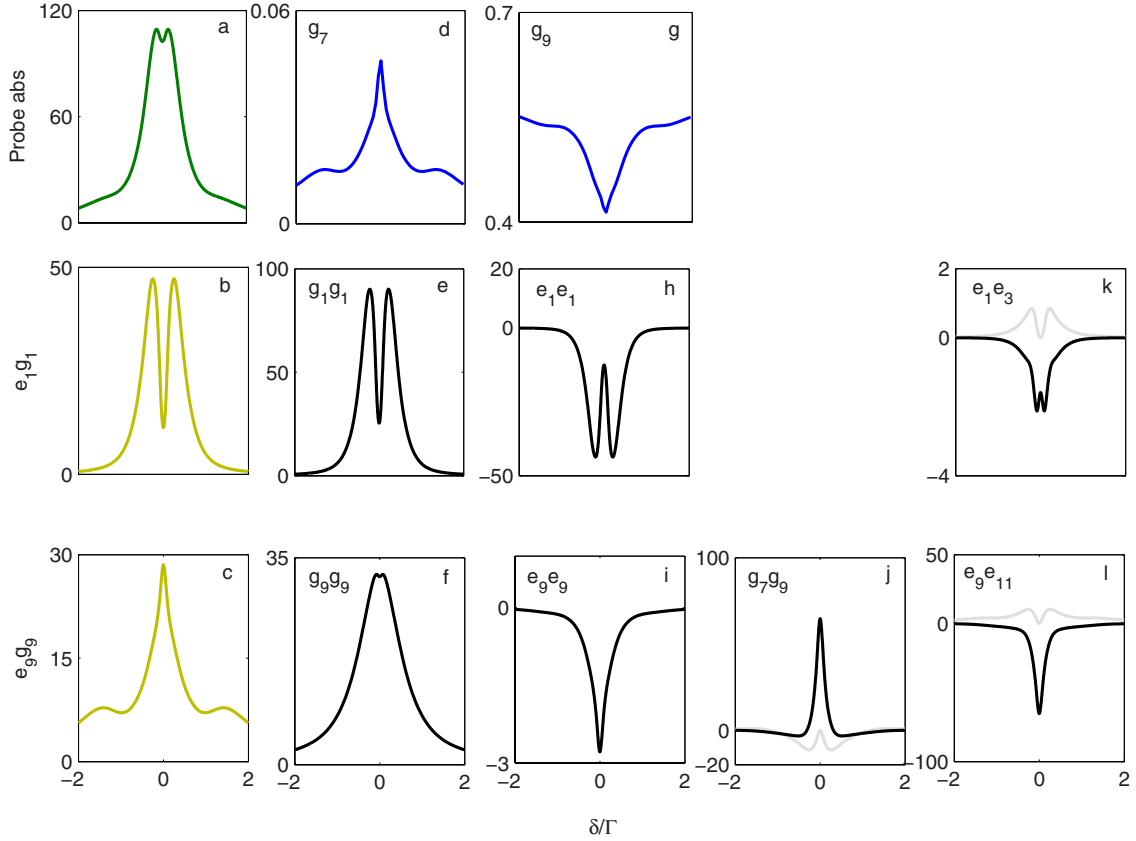


FIG. 2. (Color online) Probe absorption spectrum as a function of  $\delta/\Gamma$  for interaction of a  $F_g=4 \rightarrow F_e=5$  transition with  $\sigma_+$ -polarized pump and  $\sigma_-$ -polarized probe lasers: (a) total probe absorption, (b) and (c) main contributions to total probe absorption spectrum from  $g_i \rightarrow e_i$ ,  $i=1,9$ , transitions; (d) spectrum of population in sublevel  $g_7$ ; (e) and (f) contributions to spectra in (b) and (c) from population in  $g_1$  and  $g_9$ ; (g) spectrum of population in sublevel  $g_9$ , (h) and (i) contribution to spectra in (b) and (c) from population in  $e_1$  and  $e_9$ ; (j) contribution to spectrum in (c) from real (black) and imaginary (gray) parts of  $g_7 g_9$  coherence; (k) and (l) contributions to spectrum in (b) and (c) from real (black) and imaginary (gray) parts of  $e_1 e_3$  and  $e_9 e_{11}$  coherences.  $\Omega_1/\Gamma=5$ ,  $\Omega_2/\Gamma=3.5$ , and  $\gamma/\Gamma=0.001$ . Absorption is in units of  $\text{cm}^{-1}$ .

described as a single  $N$  system as would be the case for  $\Omega_1 \gg \Omega_2$  [1,10]. Nevertheless, some of the contributions to the total probe and pump absorption resemble those expected for an  $N$  system which results from a combination of a  $\Lambda$  and a  $V$  system. For example, the sublevels  $g_{7,9}$  and  $e_{9,11}$  form an  $N$  system which can explain the overall shape of the total pump and probe spectra but not the behavior of the probe spectrum near line center. This can be confirmed by comparing the contributions to the probe spectrum from the  $g_9 \rightarrow e_9$  transition, and the contributions to the pump spectrum from the  $g_7 \rightarrow e_9$  and  $g_9 \rightarrow e_{11}$  transitions [see Figs. 2(c), 3(c), and 3(e)] with those from the probe and pump transitions in a pure  $N$  system, shown in Fig. 6 of [10]. It should also be noted that the population spectra of  $g_7$  and  $e_9$  [Figs. 2(d) and 3(j)] resemble the  $g_9 \rightarrow e_9$  probe and the  $g_7 \rightarrow e_9$  pump spectra (as for a  $\Lambda$  system), whereas those of  $g_9$  and  $e_{11}$  [Figs. 2(g) and 3(o)] resemble the  $g_9 \rightarrow e_{11}$  pump spectrum which is complementary to the  $g_9 \rightarrow e_9$  probe spectrum, as in a  $V$  system (for a full discussion of this comparison, see [1]).

## 2. $\Omega_2 > \Omega_1 > \Gamma$

We now turn to the case where the probe Rabi frequency is greater than the pump Rabi frequency with  $\Omega_2 > \Omega_1 > \Gamma$ .

In this case, the population is swept toward the left when the probe is at resonance and swept toward the right when the probe is away from resonance, so that almost all the transitions contribute to the total spectra to some extent. The extreme left ( $g_1 \rightarrow e_1$ ) is the most populated transition at resonance and the extreme right ( $g_9 \rightarrow e_{11}$ ) transition is the most populated away from resonance, as shown in Figs. 4(b) and 4(c) and Figs. 5(b) and 5(c). In Fig. 4(a), we plot the total probe absorption spectrum which is characterized by an EIA peak at line center. The main contribution to the total probe absorption is from the  $g_1 \rightarrow e_1$  transition shown in Fig. 4(d) with a smaller contribution from the  $g_2 \rightarrow e_2$  transition (not shown). The contributions to the  $g_1 \rightarrow e_1$  probe absorption are calculated from Eq. (10) and are shown in Figs. 4(e)–4(g). We see that the main contribution to the peak at line center comes from the population in the  $g_1$  sublevel, shown in Fig. 4(e) whose effect is reduced by the contributions from the excited-state population and coherence which exhibit behavior complementary to that of the ground-state population.

In Fig. 5(a), we plot the pump absorption spectrum. The pump spectrum is a mirror image of the probe spectrum and, unlike the previous case, is characterized by a dip at line center called TWT [6]. The main contribution to the total

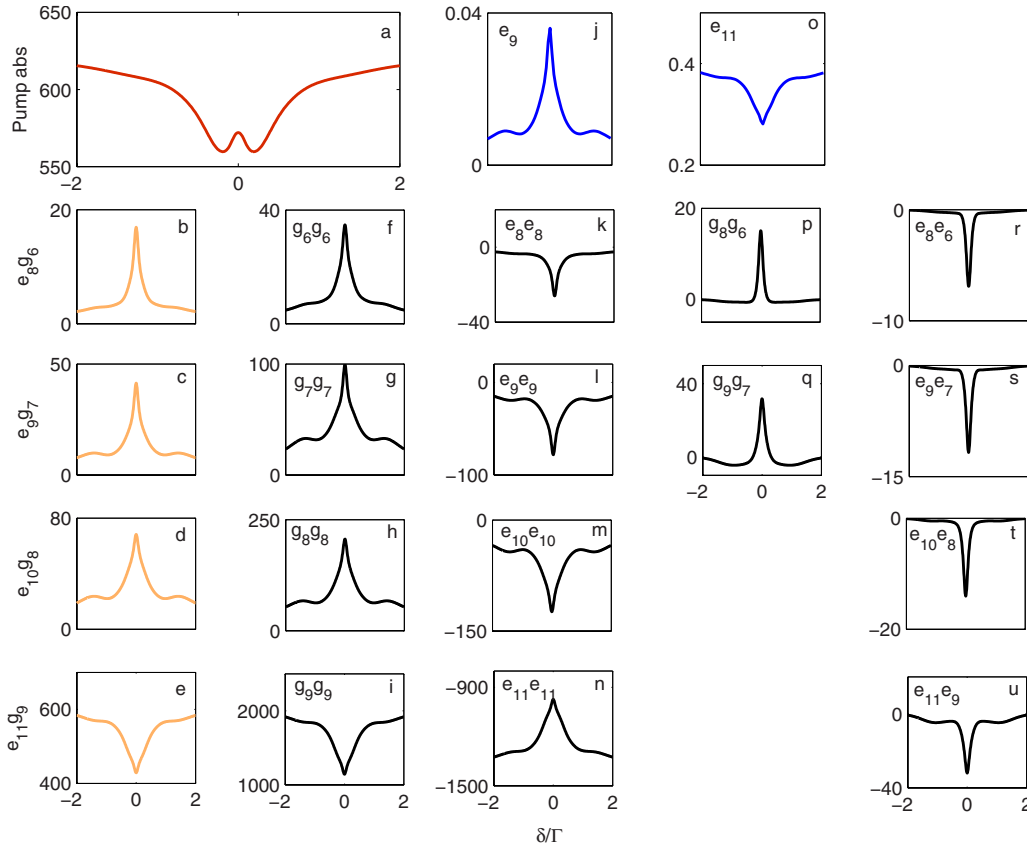


FIG. 3. (Color online) Pump absorption spectrum as a function of  $\delta/\Gamma$  for interaction of a  $F_g=4 \rightarrow F_e=5$  transition with  $\sigma_+$ -polarized pump and  $\sigma_-$ -polarized probe lasers: (a) total pump absorption; (b)–(e) contribution to total pump absorption spectrum from  $g_i \rightarrow e_{i+2}$ ,  $i=6-9$ , transitions; (f)–(i) contribution of population in sublevels  $g_i$ ,  $i=6-9$ , to spectra in (b)–(e); (j) spectrum of population in sublevel  $e_9$ ; (k)–(n) contributions of population in sublevels  $e_i$ ,  $i=8-11$ , to spectra in (b)–(e); (o) spectrum of population in sublevel  $e_{11}$ ; (p) and (q) contributions of real part of Zeeman coherence  $g_{i+2}g_i$ ,  $i=6-7$ , to spectra in (b) and (c); (r)–(u) contribution of real part of Zeeman coherence  $e_{i+2}e_i$ ,  $i=6-9$  to spectra in (b)–(e). Parameters and units as in Fig. 2.

pump absorption comes from the  $g_9 \rightarrow e_{11}$  transition, shown in Fig. 5(d). This transition is analyzed using Eq. (9) and the various contributions are shown in Figs. 5(e)–5(g). The main contribution comes from the population in  $g_9$ , which contributes a dip at line center. Again, the contributions from the excited-state population and coherence counteract that of the ground-state population.

The probe and pump spectra for this case are mirror images of each other just as one would expect for a  $V$  system (see Fig. 5 of [10]), so that, in a sense, this degenerate two-level system behaves like an effective  $V$  system, consisting of sublevels  $g_{1,9}$  and  $e_{1,11}$ .

When we exclude TOC, in an attempt to establish its role in determining the spectra, we find that all the sharp features in the pump and probe spectra of Figs. 2–5 disappear. This is in keeping with the claim [4,5] that the sharp EIA features that occur at line center in probe absorption spectra when  $\Omega_1 \gg \Omega_2 < \Gamma$  derive from TOC; in the absence of TOC, the EIA peaks turn into EIT dips. When we compare Figs. 3(a) and 5(a), we see that the width of the sharp features at line center increases with increasing probe intensity, as was found experimentally [6]. We also see that the width of the narrow features is approximately one order of magnitude

smaller than that of the broad features which is equal to the natural linewidth, as in Fig. 3 of the experimental paper.

### B. $F_g=4 \rightarrow F_e=5$ transition interacting with $\sigma_+$ -polarized pump and $\pi$ -polarized probe

We now turn to the case of a  $\sigma_+$  pump and a  $\pi$  probe, shown in Fig. 6. It was shown experimentally that for these polarizations, there is no switch over from AWT to TWT with increasing probe intensity. In order to explain this phenomenon, we calculate the probe and pump absorption spectra for a case where  $\Omega_2 \gg \Omega_1 > \Gamma$ , namely,  $\Omega_1/\Gamma=5$  and  $\Omega_2/\Gamma=14$ . The total probe absorption spectrum, shown in Fig. 6(a), is characterized by a small dip. The main contributions to the total probe absorption which come from the  $g_j \rightarrow e_i$  transitions, where  $i=j+1=5-8$ , are plotted in Figs. 6(b) and 6(c). We note that the transitions toward the center of the level diagram are characterized by a dip [Fig. 6(b)] while those toward the right are characterized by a peak [Fig. 6(c)], resulting in a net dip. The total pump spectrum, which still has an AWT despite the intense probe, is shown in Fig. 6(d), and the main contributions to it are plotted in Figs. 6(e) and 6(f). In contrast to the probe spectrum, the transitions

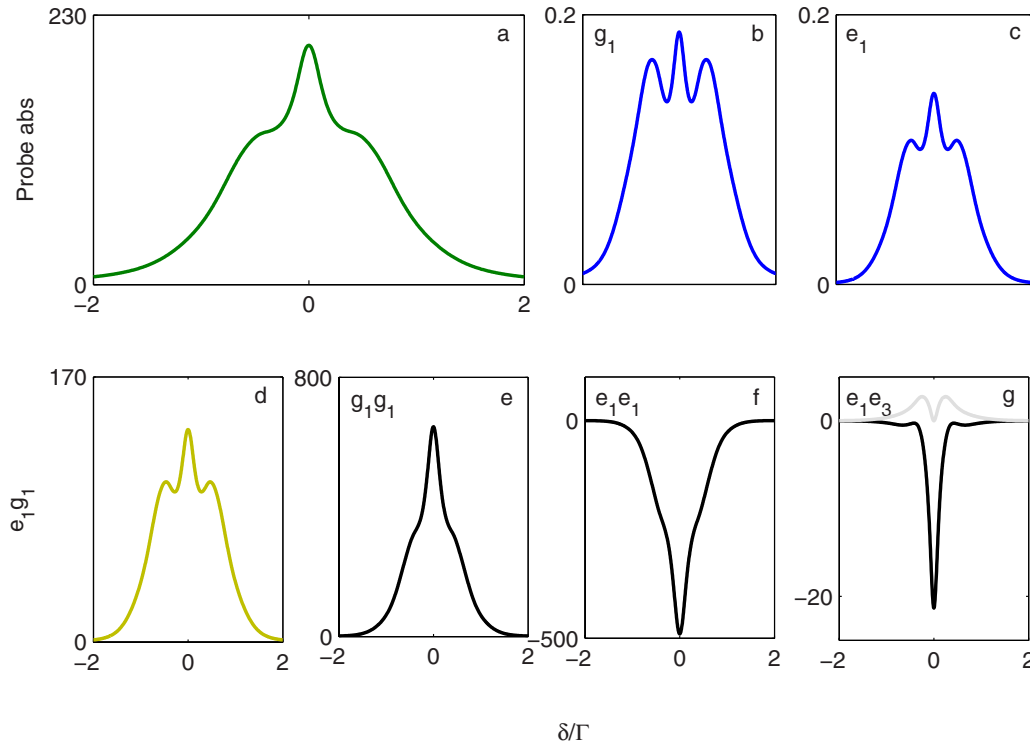


FIG. 4. (Color online) Probe absorption spectrum as a function of  $\delta/\Gamma$  for interaction of a  $F_g=4 \rightarrow F_e=5$  transition with  $\sigma_+$ -polarized pump and  $\sigma_-$ -polarized probe lasers: (a) total probe absorption; (b) spectrum of population in sublevel  $g_1$ ; (c) spectrum of population in sublevel  $e_1$ ; (d) contribution to total probe absorption spectrum from  $g_1 \rightarrow e_1$  transition; (e) contribution of population in sublevel  $g_1$  to spectrum in (d); (f) contribution of population in sublevels  $e_1$  to spectrum in (d); (g) contribution of real (black) and imaginary (gray) part of Zeeman coherence  $e_1 e_3$  to (d).  $\Omega_1/\Gamma=5$ ,  $\Omega_2/\Gamma=6.3$ , and  $\gamma/\Gamma=0.001$ . Absorption is in units of  $\text{cm}^{-1}$ .

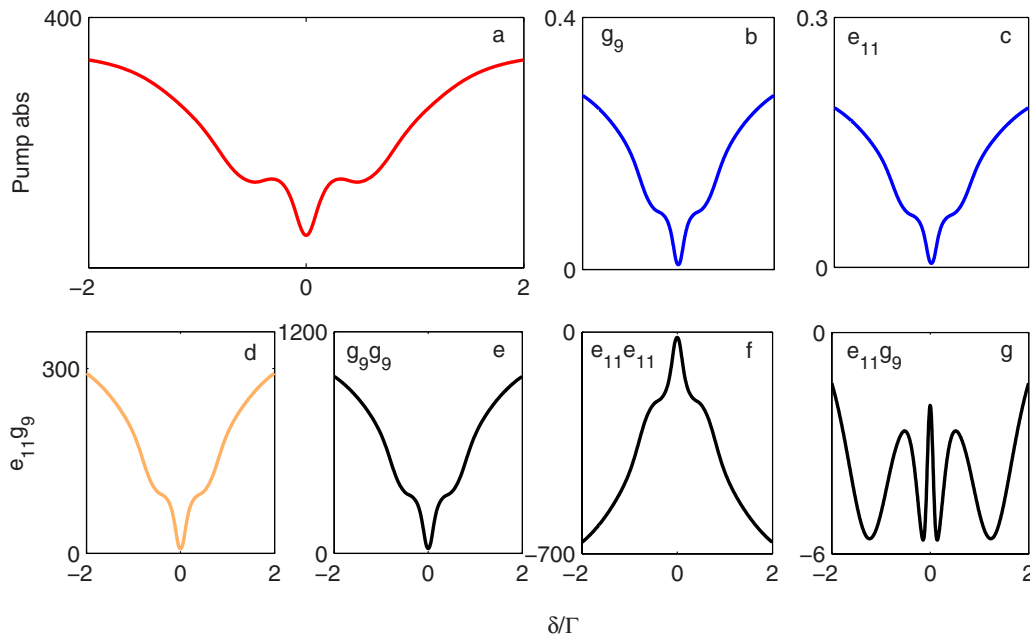


FIG. 5. (Color online) Pump absorption spectrum as a function of  $\delta/\Gamma$  for interaction of a  $F_g=4 \rightarrow F_e=5$  transition with  $\sigma_+$ -polarized pump and  $\sigma_-$ -polarized probe lasers: (a) total pump absorption; (b) spectrum of population in sublevel  $g_9$ ; (c) spectrum of population in sublevel  $e_{11}$ ; (d) contribution to total pump absorption spectrum from  $g_9 \rightarrow e_{11}$  transition; (e) contribution of population in sublevel  $g_9$  to spectrum in (d); (f) contribution of population in sublevel  $e_{11}$  to spectrum in (d); (g) contribution of real part of Zeeman coherence  $e_{11} e_9$  to spectrum in (d). Parameters and units as in Fig. 4.

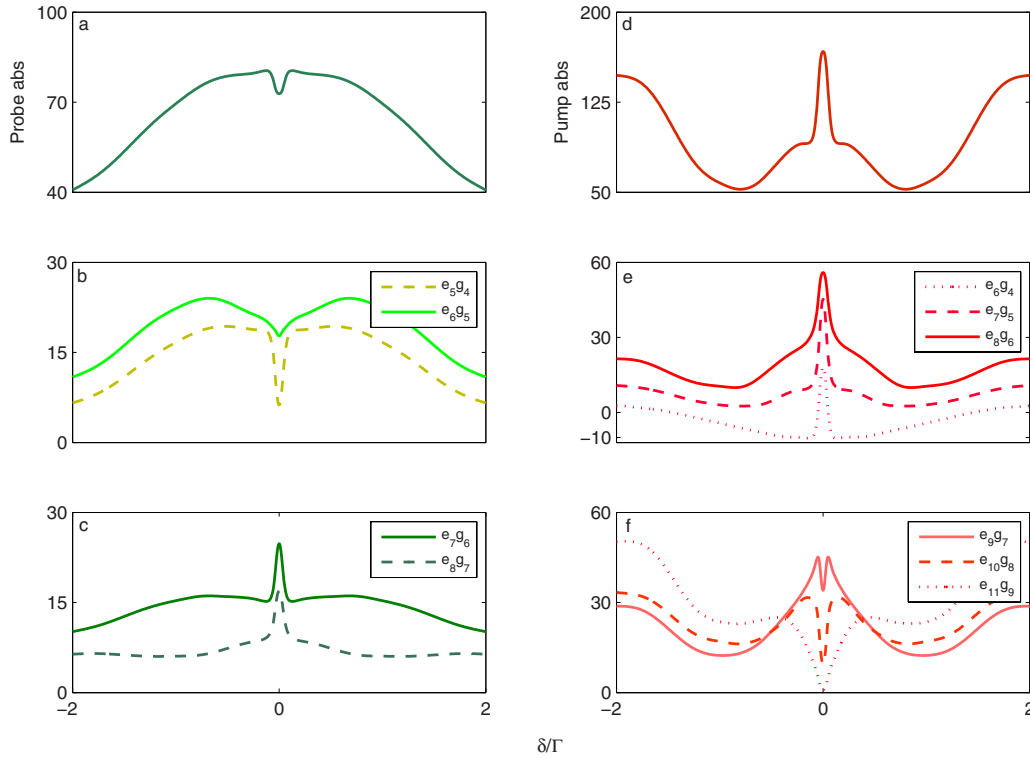


FIG. 6. (Color online) Probe and pump absorption spectrum as a function of  $\delta/\Gamma$  for interaction of a  $F_g=4 \rightarrow F_e=5$  transition with  $\sigma_+$ -polarized pump and  $\pi$ -polarized probe lasers: (a) total probe absorption; (b) contribution to total probe absorption spectrum from  $g_i \rightarrow e_{i+1}$ ,  $i=4-5$ , transitions characterized by a dip; (c) contribution to total probe absorption spectrum from  $g_i \rightarrow e_{i+1}$ ,  $i=6-7$ , transitions characterized by a peak; (d) total pump absorption; (e) contribution to total pump absorption spectrum from  $g_i \rightarrow e_{i+1}$ ,  $i=4-6$ , transition characterized by a peak; (f) contribution to total pump absorption spectrum from  $g_i \rightarrow e_{i+1}$ ,  $i=7-9$ , transition characterized by a dip.  $\Omega_1/\Gamma=5$ ,  $\Omega_2/\Gamma=14$ , and  $\gamma/\Gamma=0.001$ . Absorption is in units of  $\text{cm}^{-1}$ .

which are toward the center of the level diagram contribute a peak at line center [see Fig. 6(e)] while those that are closer to the right contribute a dip [Fig. 6(f)], resulting in an overall peak. It can be shown that, in the absence of TOC due to the population of the excited sublevels, the probe spectrum has an overall dip rather than a peak. As the probe intensity increases even further, the population concentrates even more in the center of the system and the excited states become more populated. Even for very high probe intensities the population is never swept to the extreme left and right transitions, as in the case of a  $\sigma_-$ -polarized probe. Thus the pump spectrum never exhibits a changeover to TWT.

#### IV. CONCLUSIONS

In this paper, we studied the absorption spectra for an intense pump and a probe of comparable intensity interacting with the  $F_g=4 \rightarrow F_e=5$  transition in the  $D_2$  line of  $^{133}\text{Cs}$  in an atomic beam. The aim was to reproduce and analyze the experimental findings of Dahl *et al.* [6] who studied this system for several combinations of pump and probe polarizations. Essentially, they found that the pump absorption spectrum has an AWT structure for all relative values of the pump and probe Rabi frequencies studied, except for the combination of a  $\sigma_+$ -polarized pump and a  $\sigma_-$ -polarized probe, where there is a changeover from AWT to TWT behavior when the probe intensity becomes greater than that of

the pump. In order to understand the reasons for this difference in behavior, we analyzed two contrasting polarization combinations, a  $\sigma_+$ -polarized pump and a  $\sigma_-$ -polarized probe where the changeover occurs, and a  $\sigma_+$ -polarized pump and a  $\pi$ -polarized probe where no changeover is observed even at very high probe intensities. We used the same approach as in [1] for calculating and analyzing the spectra.

We first analyzed the case of a resonant  $\sigma_+$ -polarized pump and a tunable  $\sigma_-$ -polarized probe, shown in Fig. 1(a), where  $\Omega_2 < \Omega_1$ , and the absorption spectrum is characterized by an AWT. We found that most of the population is swept to the right of the level diagram when the probe is detuned from resonance, but at resonance, other sublevels toward the left of the diagram are also populated. Indeed, the small dip at line center in the probe absorption can be shown to derive from the transition at the extreme left of the diagram. Although this case cannot be simulated as a pure  $N$  system [10], as would be the case if the probe were much weaker than the pump [1], the pump absorption spectrum resembles that expected for an  $N$  system. We then considered the case  $\Omega_2 > \Omega_1$  where the pump absorption spectrum has a TWT structure and the probe spectrum is the mirror-image of that of the pump, displaying an EIA peak at line center. For this case, the population is swept toward the left at resonance and toward the right away from resonance. This system can be considered as an effective  $V$  system formed by the transitions at the extreme left and right of the level diagram.

We then examined the case of a  $\sigma_+$ -polarized pump and a  $\pi$ -polarized probe, where the pump absorption exhibits an AWT structure even for very high probe intensities. At high probe intensity, the population is never completely swept either to the right or to the left at any detuning, as in the case of  $\sigma_-$ -polarized probe, but is spread over a number of transitions near the center of the system, populating both the ground and excited sublevels. For this reason, a switchover to a TWT structure does not occur. The sum of the contributions to the spectra leads to an overall dip at line center in the probe spectrum and an AWT structure for the pump spec-

trum. For all the cases studied, we note that the pump and probe spectra show complementary behavior [1,11], and that the sharp features in the pump and probe spectra derive from TOC [4,5]. We also note that the shape of the individual contributions to the spectra are influenced by the absolute and relative intensities of the pump and probe.

#### ACKNOWLEDGMENT

We thank Katrin Dahl for providing us with experimental data.

- 
- [1] T. Zigdon, A. D. Wilson-Gordon, and H. Friedmann, Phys. Rev. A **77**, 033836 (2008).  
[2] A. M. Akulshin, S. Barreiro, and A. Lezama, Phys. Rev. A **57**, 2996 (1998).  
[3] A. Lezama, S. Barreiro, and A. M. Akulshin, Phys. Rev. A **59**, 4732 (1999).  
[4] A. V. Taichenachev, A. M. Tumaikin, and V. I. Yudin, Phys. Rev. A **61**, 011802(R) (1999).  
[5] C. Goren, A. D. Wilson-Gordon, M. Rosenbluh, and H. Friedmann, Phys. Rev. A **67**, 033807 (2003).  
[6] K. Dahl, L. Spani Molella, R.-H. Rinkleff, and K. Danzmann, Opt. Lett. **33**, 983 (2008).  
[7] L. Spani Molella, R.-H. Rinkleff, and K. Danzmann, Phys. Rev. A **72**, 041802(R) (2005).  
[8] R. W. Boyd, *Nonlinear Optics*, 2nd ed. (Academic, San Diego, 2003).  
[9] E. D. Clercq, M. D. Labachellerie, G. Avila, P. Cerez, and M. Tetu, J. Phys. **45**, 239 (1984).  
[10] C. Goren, A. D. Wilson-Gordon, M. Rosenbluh, and H. Friedmann, Phys. Rev. A **69**, 053818 (2004).  
[11] H. Friedmann and A. D. Wilson-Gordon, Phys. Rev. A **36**, 1333 (1987).